IDENTIFICATION OF THE LOCAL $\sigma_{eff} - \varepsilon_{eff}$ LAW FOR CONCRETE CYLINDERS UNDER UNIAXIAL MONOTONE COMPRESSION

Elena FERRETTI [1] Filippo BASTIANINI [2]

[1] *DISTART – Department of Structures, Transports, Waters, Survey and Territory Engineering, University of Bologna, Italy*
e-mail: *elena.ferretti@mail.ing.unibo.it*

[2] *Department of Innovation Engineering, University of Lecce, Italy*
e-mail: *urco@libero.it*

Abstract

The present study is part of an identifying programme for constitutive parameters in damaged materials, termed the "effective parameters". The programme starting point is that the experimental response depends not only on constitutive parameters, but also on structural mechanics and interaction with the test-machine. In previous studies, it was showed how the load-displacement diagram of compressed concrete cylinders is affected by crack propagation, through the resistant structure modification. Moreover, it was analytically demonstrated that the effective stress (σ_{eff})-effective strain (ε_{eff}) curve exhibits a strictly positive derivative at the point corresponding to the average stress ($\bar{\sigma}$)-average strain ($\bar{\varepsilon}$) curve peak. Finally, it was proposed a new identification procedure which provided satisfactory results for cylindrical specimens of varying slendernesses, giving monotone strictly non-decreasing and size-effect insensitive $\sigma_{eff} - \varepsilon_{eff}$ curves. In the present paper, the proposed identification procedure is tested on specimens of the same geometry, but with different failure mechanisms.

Key words: *identification, constitutive parameters, concrete, crack propagation, experimental acquisitions*

1 Introduction

In order to derive a constitutive law in uniaxial compression from experimental data, it is common practice to define the average stress $\bar{\sigma}$ and the average strain $\bar{\varepsilon}$ as shown in Fig. 1. The $\bar{\sigma}$-$\bar{\varepsilon}$ relationship in Fig. 1 is known as uniaxial constitutive law for monotone strain processes. The term "constitutive" is associated with the $\bar{\sigma}$-$\bar{\varepsilon}$ relationship since this relationship is considered as representative of the mechanic behaviour of the material. However, one can make the following remarks concerning the choice of this term:

- The $\bar{\sigma}$-$\bar{\varepsilon}$ law in Fig. 1 is size-effect sensitive, while a constitutive law should not exhibit a size effect.
- The identification procedure in Fig. 1 consists of a mere change of scale. Thus, experimental and identified curves are homothetic (Fig. 1). In particular, they both exhibit

a softening behaviour. The softening behaviour in the $N-v$ relationship has a well known physical meaning, linked to the structure instability. On the contrary, it is not possible to associate a physical meaning with the softening behaviour of a material response ($\bar{\sigma}-\bar{\varepsilon}$ relationship), as the concept of instability loses its sense in the infinitesimal neighbourhood of a point (Ref. [1]). Besides, from the beginning of the 20th century forth, strain-softening has been widely regarded as inadmissible by several authors (Ref. [2]).

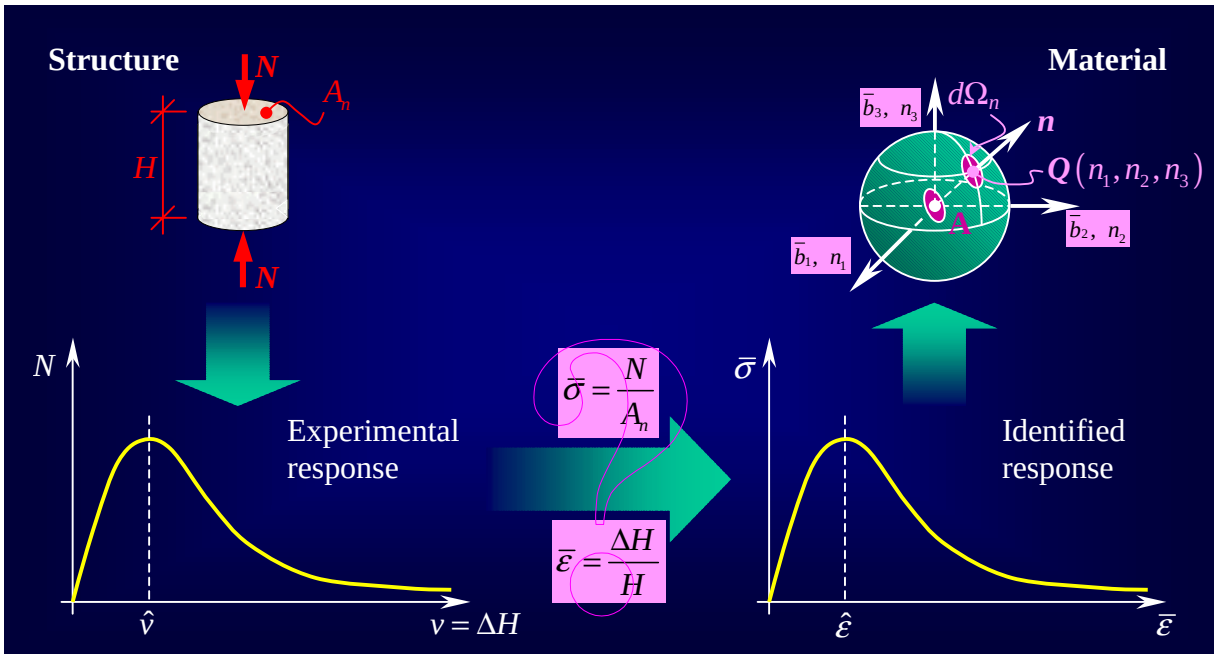

Figure 1: Traditional identification of mono-axial constitutive law by experimental tests.

No exhaustive explanation for these inconsistencies has been provided by the traditional identification procedure. In Ref. [1] they are related to the impossibility of performing mechanical tests on the material directly: the object in testing is never the material, but a specimen, that is to say, a structure interacting with the test-machine (Fig. 1). Thus, experimental results univocally characterise the behaviour of the specimen-test machine system, and not of the material. In other words, the softening branch has a meaning that is only linked to the structural instability. This branch cannot provide information on the material constitutive behaviour, but through an identifying model.

To identify the constitutive laws starting from the experimental results it is necessary to evaluate all factors influencing a test result (Ref. [1]). Indeed, since the specimen is a structure interacting with the test-machine, the experimental results (R) depend not only on the constitutive properties (C), as shown in Fig. 2, but also on the structural mechanics (S), the interactions between test-machine and specimen (I), and the test-machine metrological characteristics (M):

$$R = C + S + I + M \ . \tag{1}$$

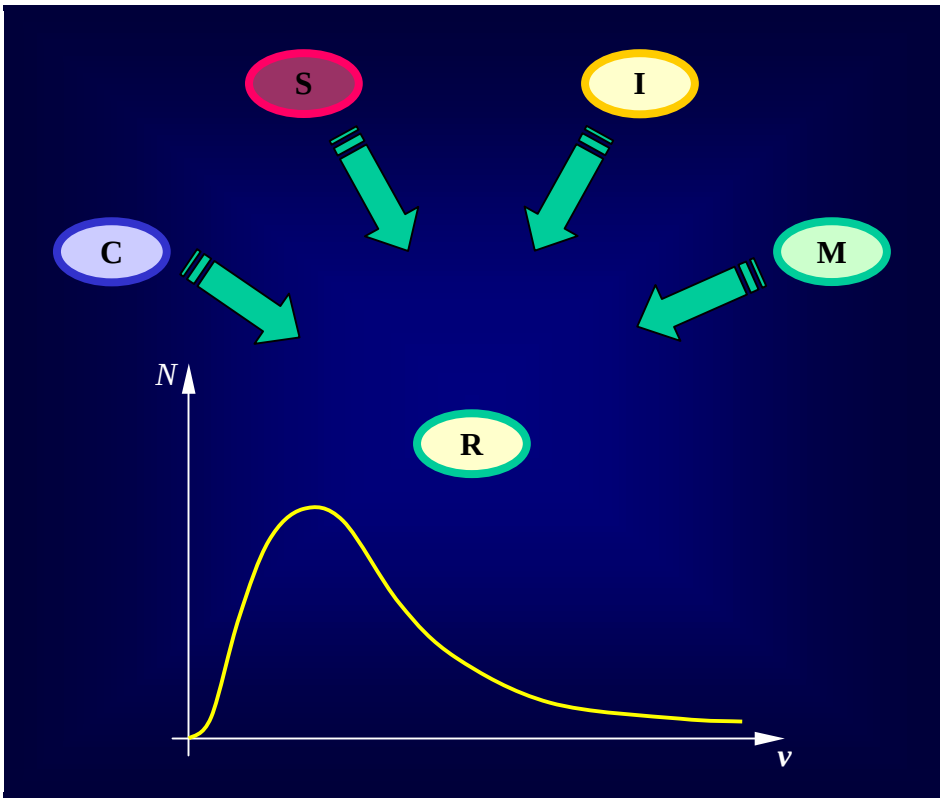

Figure 2: Factors influencing the experimental results.

On the base of partially analogous considerations, Rosati et. al. (Ref. [4]) have recently proposed a complete response for concrete loaded in tension.

It is then necessary to define an identifying procedure from experimental data to material behaviour (inverse problem), which is not affected by the remarks concerning the approach in Fig. 1.

A proposal for concrete in monotone uniaxial compression is given in Ref. [5]. In the present paper, an experimental validation to the identifying procedure proposed in Ref. [5] is presented.

2 Identification approach of σ-ε effective behaviour in mono-axial compression

2.1 Identification of the effective stress

Name K_C, K_S, K_I, and K_M the weighed contributions assumed by C, S, I, and M, respectively, in the definition of R (Eq. (1)):

$$C = K_C R\,, \qquad S = K_S R\,, \qquad I = K_I R\,, \qquad M = K_M R\,. \tag{2}$$

Substituting the above equalities in Eq. (1), one can obtain a condition of norm to one for the sum of all the weighed contributions:

$$K_C + K_S + K_I + K_M = 1. \tag{3}$$

All the contributions but the constitutive behaviour can be grouped in a single factor K:

$$K = K_S + K_I + K_M . \tag{4}$$

The position in Eq. (4) allows us to replace the relationship following from the identifying procedure in Fig. 1:

$$C \equiv R , \tag{5}$$

with the following relationship:

$$C = (1 - K) R . \tag{6}$$

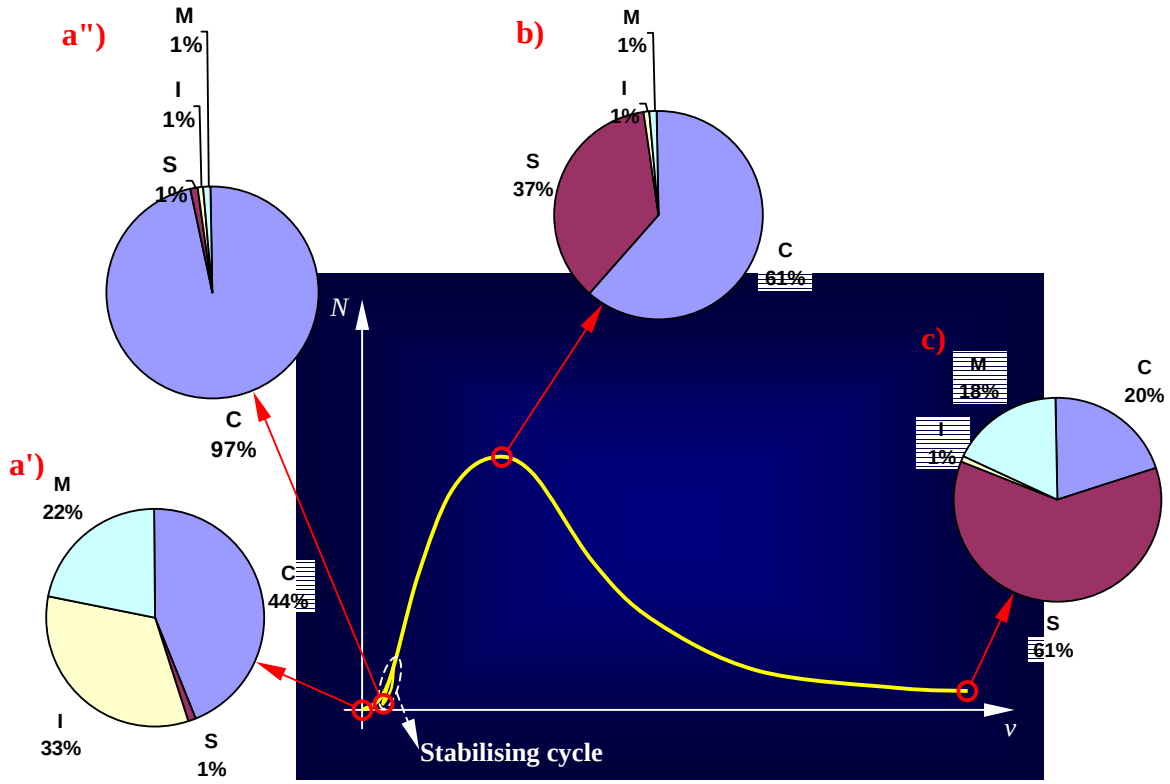

Figure 3: Qualitative repartition of R at the beginning without stabilising cycle (a'), at the beginning with stabilising cycle (a"), at an intermediate load step (b), and at the end of the test (c).

By means of Eq. (6), it is possible to evaluate the constitutive properties, taking into account the behaviour of the specimen-test machine system, which is represented by the parameter K.

This approach is formally more correct than the approach leading to Eq. (5). Nevertheless, it is not of immediate use for identifying constitutive properties, since $K_C = K_C(R)$, $K_S = K_S(R)$, $K_I = K_I(R)$, and $K_M = K_M(R)$ are, generally speaking, load-step functions. That is to say,

$$K = K(R) \tag{7}$$

is a load-step function, and not a constant of the performing test.

The variation law of *K* is not known a priori. A plausible repartition of *R* at the beginning without stabilising cycle (a'), at the beginning with stabilising cycle (a"), at an intermediate load step (b), and at the end of the test (c) is given in Fig. 3. It must be incidentally recalled that a stabilising cycle is an unloading-reloading cycle effectuated for a preloading equal to about the 10% of the maximal presumed load. The stabilising cycle is done in order to limit the influence of the specimen-test machine interaction and test-machine metrological properties on the experimental result.

In conclusion, it is not possible to establish a homothetic correspondence between the experimental load-displacement relationship and the uniaxial constitutive stress-strain relationship. Moreover, since Eq. (7) is not of objective determination, *K* can only be estimated, with regard to the material scale. This involves the identification of an effective response, and not of a constitutive response in its rigorous meaning.

The main consequence of Eqs (6, 7) is the loss of the traditional identity between the experimental and the effective curve shape. In other words, the effective curve may not exhibit the typical softening behaviour of the experimental curve. Since it is impossible to associate a physical meaning with the strain-softening behaviour of a material response, one can rightly expect that the identified effective laws is monotone nondecreasing for any material.

An analysis of the reciprocal ratios between K_C, K_S, K_I, and K_M for compressed concrete cylinders (Ref. [1]) showed that it is possible to assume $K \cong K_S$. Thus, the large structural scheme variation of concrete cylinders, following from the propagation of dominant bi-cone shaped cracks (Fig. 4c), is preponderant in comparison to the other addends in Eq. (4). As shown in Fig. 4c, the failure mechanism of concrete cylinders isolates an internal core, in which crack propagation never occurred, and a volume of incoherent material. This involves a resistant structure with modifying geometry at a general load step.

To identify the scale factor of the σ axis with respect to the *N* axis (Fig. 1), it is fundamental to introduce a parameter whose dimensions are those of an area and whose incremental law, in the assumption that $K \cong K_S$, is linked to the structural scheme variation. In Ref. [1], this parameter has be termed the resistant area A_{res}, as to indicate that this area is a quantity depending from the variation of resistant structure.

In Ref. [1], it was proposed to estimate the resistant area A_{res} in accordance with the Fracture Mechanics with Damage:

$$A_{res} = A_n(1-D), \tag{8}$$

where D is a scalar.

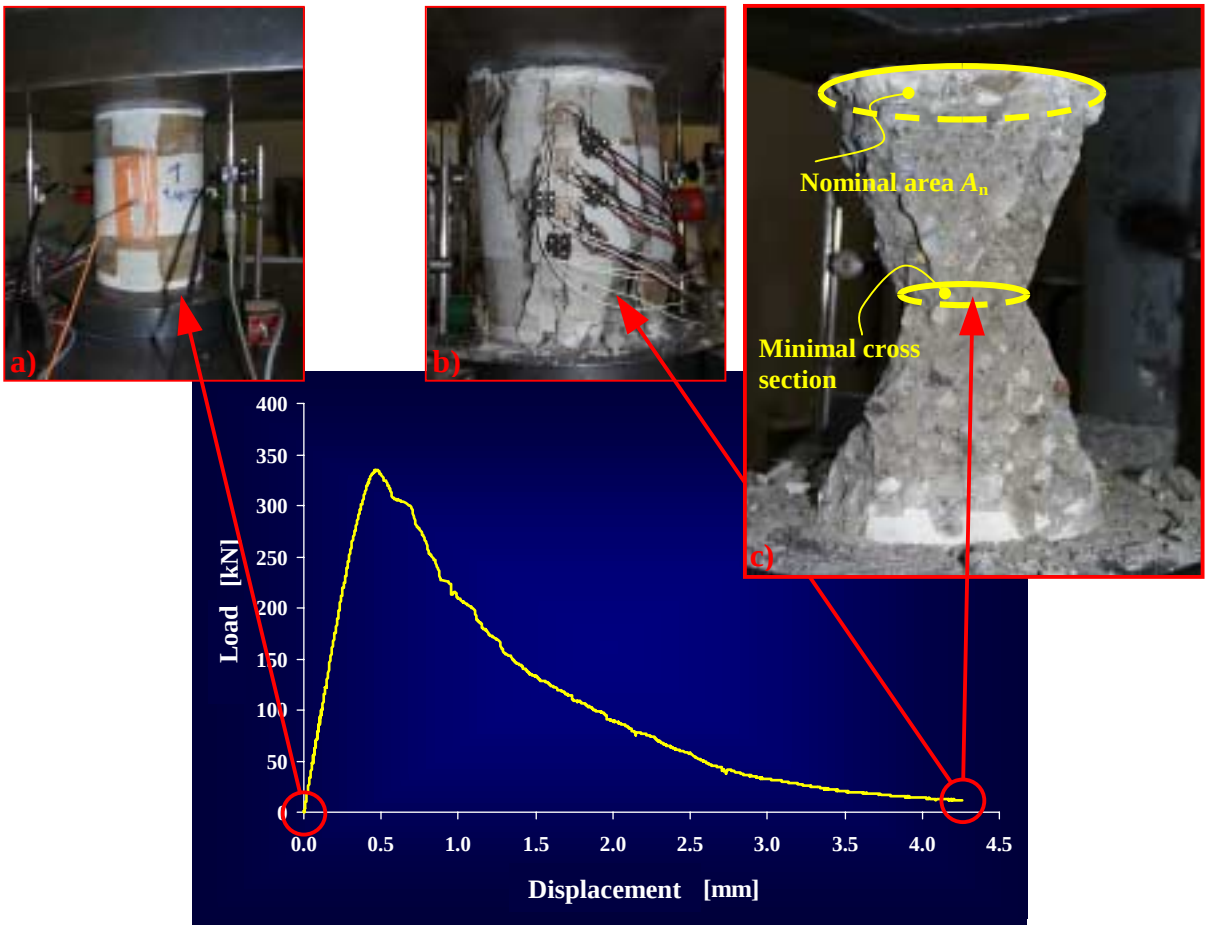

Figure 4: Aspect of the concrete specimen at the beginning of the test (a), at the end of the test (b), and after the removal of all the incoherent material (c).

In accordance with Eq. (8), the effective stress has then been defined as the average stress acting on the area A_{res} :

$$\sigma_{eff} = \frac{N}{A_{res}}. \tag{9}$$

Alternatively, the effective stress can be expressed as:

$$\sigma_{eff} = \bar{\sigma}\frac{A_n}{A_{res}}. \tag{10}$$

The analogy with the manner of operation of the Fracture Mechanics with Damage is limited to Eq. (8). Indeed, in the Fracture Mechanics with Damage, D has an analytic formulation and

is considered as uniformly distributed on A_n. In Ref. [1], $D = D(R)$ is experimentally evaluated and all the damage is considered as localised in the volume of incoherent material.

2.1.1 Identification of the damage law

To evaluate $D = D(R)$, two experimental damage laws were employed in Ref. [1]. The first damage law, D_1 (Ref. [6]), relates the damage to the percentage variation of the microseismic signal velocity V at the current point (set-up of the microseismic test in Fig. 5.a):

$$D_1 = 1 - \frac{V}{V_0}, \tag{11}$$

where V_0 is the initial microseismic signal velocity.

The second damage law, D_2 (Ref. [7]), relates the damage to the dissipated energy W_d at the current point (Fig. 5.b):

$$D_2 = \frac{W_d}{W_{d,t}}, \tag{12}$$

where $W_{d,t}$ is the total dissipated energy. The evaluation of W_d has been done in accordance with the experimental unloading law.

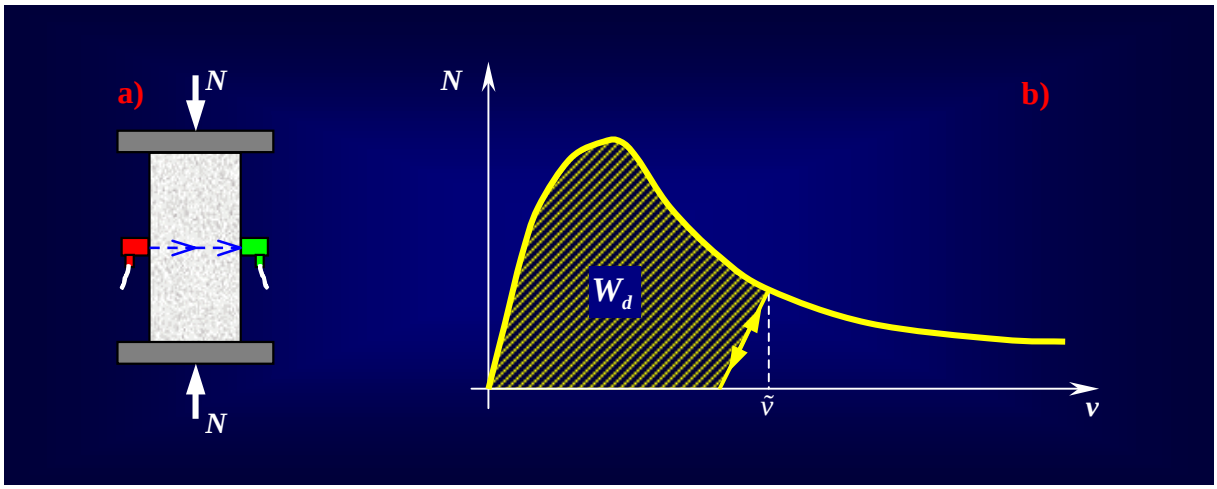

Figure 5: a) Test set-up for the identification of D_1; b) Evaluation of W_d for the identification of D_2.

D_1 and D_2 turned out to be very close to each other (Ref. [1]). To identify the effective properties, only the D_2 damage law has been used in Ref. [1], since this law is not affected by limitations in the survey field. On the contrary, starting from a certain load step, the damage parameter D_1 is affected by the noise of the crack propagation so much as to cannot appreciate any longer its variation.

In Ref. [1], also the specimen defects at the natural state, through the amount of initial damage D_0, have been evaluated. To take into account also the amount of initial damage, the Eq. (8) has been modified as follows:

$$A_{res} = A_n \left(1 - D_{eq}\right), \tag{13}$$

where D_{eq} is the equivalent damage, comprehensive both of the initial damage D_0 and the damage D_2 due to the monotone loading. D_{eq} can be expressed as:

$$D_{eq} = 1 - \left(1 - D_0\right)\left(1 - D_2\right) = D_0 + D_2 - D_0 D_2 . \tag{14}$$

The nominal area deprived of the defects at the natural state, termed the reduced nominal area A_n', results from:

$$A_n' = A_n \left(1 - D_0\right). \tag{15}$$

2.1.2 Algebraic considerations about the formulation of the effective stress

In Ref. [5], an interesting information about the sign of the effective stress derivative in the σ_{eff} - $\bar{\varepsilon}$ plane is provided, directly rising from the formulation of the effective stress in Eq. (9).

In particular, it has been analytically demonstrated how a point with strictly positive tangent in the $\sigma_{eff} - \bar{\varepsilon}$ curve corresponds to the point with zero tangent in the $N - v$ curve. This is a notable result, since it has been obtained without having introduced any other assumptions on the shape of the damage law except the physically justifiable condition of non zero tangent in correspondence of the maximal load.

As regards the sign of the tangent in the $\sigma_{eff} - \bar{\varepsilon}$ plane for $v > \hat{v}$, this depends on the value of the ratio ρ, defined as follows:

$$\rho = \frac{N' A_{res}}{N A_{res}'}, \tag{16}$$

where the superscript indicates derivation with respect to the variable *v*.

It results:

$$\frac{d\sigma_{eff}}{d\bar{\varepsilon}} \geq 0 \qquad \forall v > \hat{v},\ 0 \leq \rho \leq 1 \tag{17'}$$

$$\frac{d\sigma_{eff}}{d\bar{\varepsilon}} < 0 \qquad \forall v > \hat{v},\ \rho > 1 . \tag{17''}$$

In alternative to Eqs (17), one can study the sign for $v > \hat{v}$ of the derivative of *q*, defined as follows:

$$q = \frac{\bar{\sigma}_{\max}}{\sigma_{eff}} \overset{(8)}{=} \frac{A_{res}}{A_n} \Big/ \frac{N}{N_{\max}}, \tag{18}$$

in which the function q has been expressed as the ratio between the normalised resistant area and the normalised load. It follows that:

$$q' = -\bar{\sigma}_{\max} \frac{\sigma'_{eff}}{\sigma^2_{eff}} = -\bar{\sigma}_{\max} \frac{N' A_{res} - N A'_{res}}{N^2}. \tag{19}$$

From Eq. (19) it can be observed that the sign of q' too is determined by the ratio ρ. The result is:

$$q' > 0 \qquad \forall v > \hat{v},\ \rho > 1; \tag{20'}$$

$$q' \le 0 \qquad \forall v > \hat{v},\ 0 \le \rho \le 1. \tag{20''}$$

On the other hand, the sign of q' follows directly from Eqs (17) and the first equality in Eq. (19), which states that the signs of q' and σ'_{eff} are unconformable $\forall v$.

In conclusion, the sign of $d\sigma_{eff} / d\bar{\varepsilon}$ is surely positive for $0 \le v \le \hat{v}$, whereas it is only known when the damage law is known for $v > \hat{v}$.

2.2 Identification of the effective strain

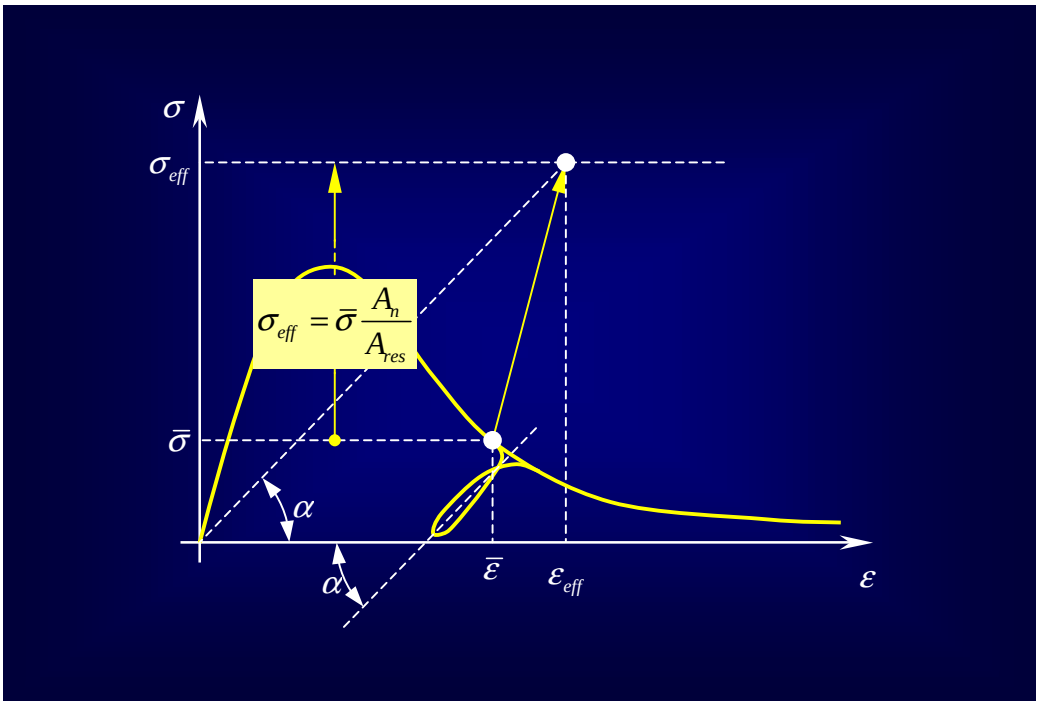

Figure 6: Identification of ε_{eff} starting from the known value of σ_{eff}.

As regards the scale factor of the ε axis with respect to the *v* axis (Fig. 1), the effective strain ε_{eff} has been identified in Ref. [1] considering that only the conservative forces act in a generic unloading-reloading cycle. In other words, these cycles should be characterised by constant values of resistant area. For this assumption, the instantaneous secant stiffness of the σ_{eff} - ε_{eff} law, $E_s = \tan\alpha$ (Fig. 6), is taken equal to the average slope of the unloading-reloading cycle at the current point. Thus, the generic point σ_{eff} - ε_{eff} results from the intersection of the two lines $\sigma = \sigma_{eff}$ and $\sigma = E_s\varepsilon$.

Figure 6 shows the identification of the effective strain ε_{eff}, starting from the value of effective stress σ_{eff}, Eqs (9, 8), and the knowledge of the damage law *D*.

3 Results of the identification procedure

The results of a first experimental programme on six cylinders of varying slenderness have been provided in Ref. [5]. The main conclusions on the $\sigma_{eff} - \varepsilon_{eff}$ identification procedure are summarised in the following points:

1) The slope of the unloading-reloading cycles is sensibly independent on the slenderness of the specimens (Fig. 7). This result supports the assumption for which the parameters characterising the unloading-reloading cycles are linked to properties of the material and do not depend on the structural mechanics. In other words, the resistant area does not change in the unloading-reloading cycles.

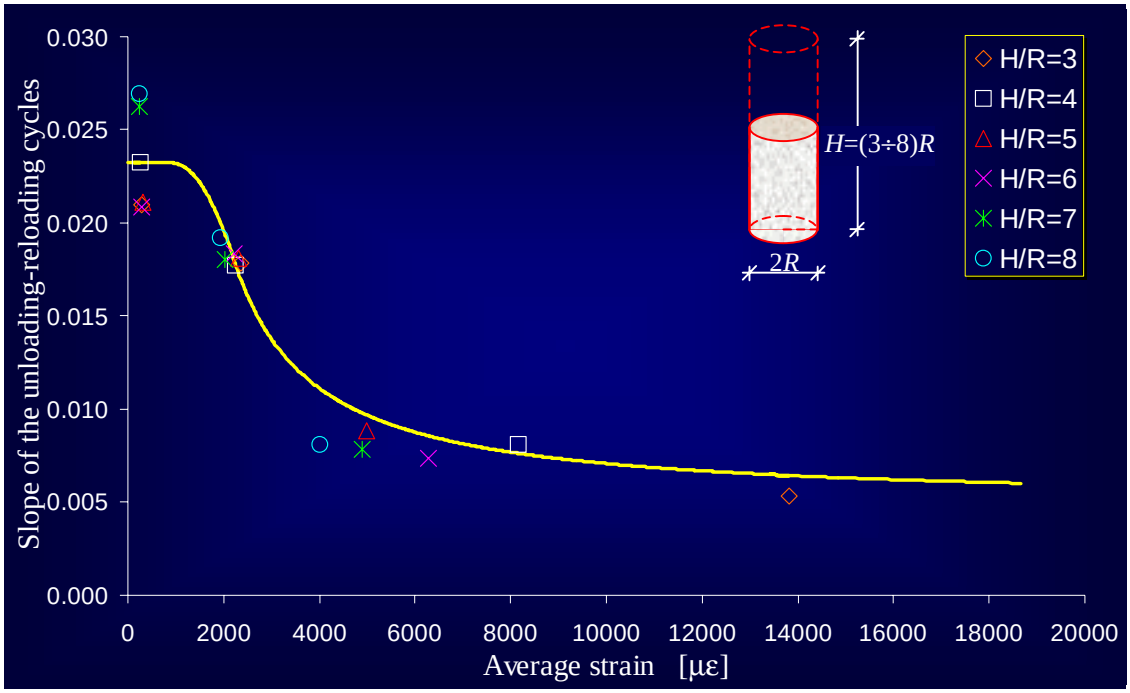

Figure 7: Interpolating law of the unloading-reloading cycles average slope variation.

2) A strictly positive derivative characterises the effective properties curves in the $\sigma_{eff} - \varepsilon_{eff}$ plane (Fig. 8). This result directly follows from the experimental $q(v)$ function, that turned out to be a positive-valued, monotone strictly nonincreasing function. This implies that the resistant area decreasing rate is faster than the load decreasing rate, for the performed tests. This circumstance and the negative sign between q' and σ'_{eff} (Eq. (19)) ensure the effective stress derivative to be positive also for $v > \hat{v}$ (Eq. 20″).

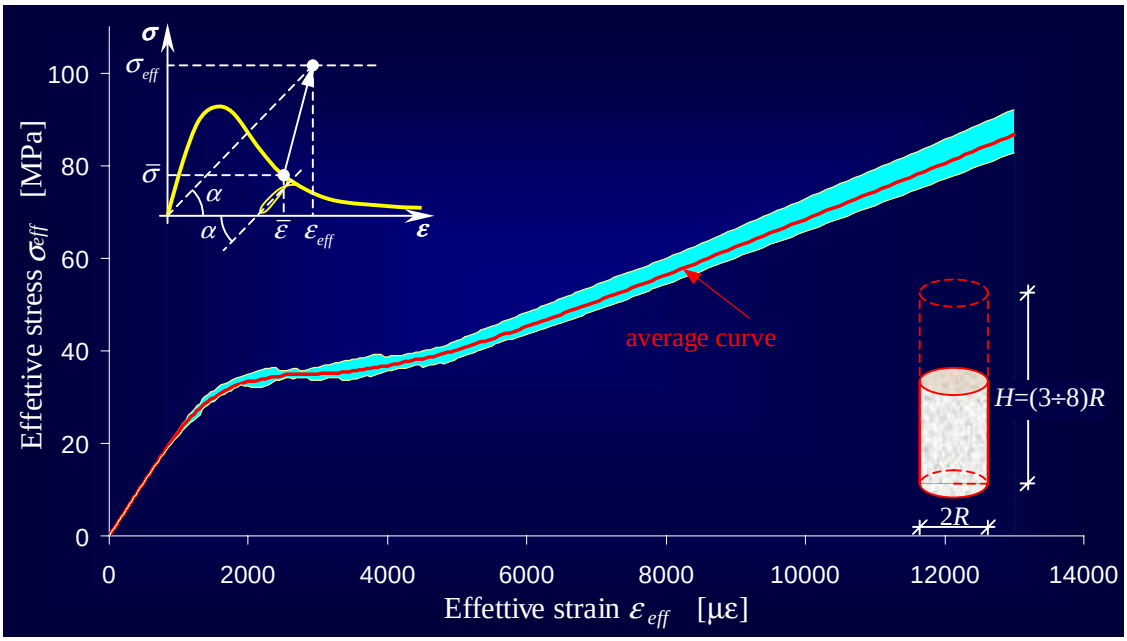

Figure 8: $\sigma_{eff} - \varepsilon_{eff}$ dispersion range for variable slenderness.

3) All the $\sigma_{eff} - \varepsilon_{eff}$ relationships obtained for the six tested geometries fall within the cyan region in Fig. 8 (dispersion range). Since the dispersion range is very little, it can be stated that the effective properties curves are size-effect insensitive.

These results allows us to assert that the two inconsistencies of the traditional identification procedure, pointed out in the introduction remarks, fall down with the new identification procedure. The $\sigma_{eff} - \varepsilon_{eff}$ relationship seems then to better represent the behaviour of the material than the $\bar{\sigma} - \bar{\varepsilon}$ relationship is able to do.

In this paper, the results of a second experimental programme are presented, as to provide a further validation to the identification procedure proposed in Ref. [1]. Also this experimental programme was performed in the intent to derive a qualitative and not quantitative information. For this reason, the number of the specimens to test was limited to two.

This second time, the geometry of the two specimens is the same, but they are forced to fail in different ways.

As well known, a concrete cylinder in uniaxial compression fails with a dominant bi-cone shaped crack which enucleates in correspondence of the press plates and propagates towards the middle cross-section. To modify the failure mechanism, one of the two specimens was cut along its middle cross-section. Before restoring the specimen, three grommets were fixed on the middle cross-section (Fig. 9).

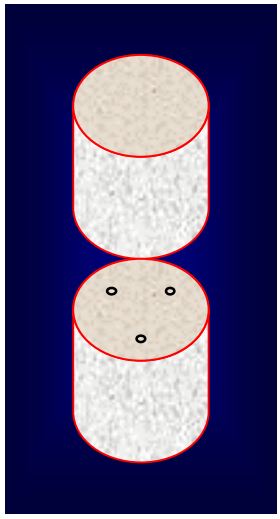

Figure 9: Positioning of the three grommets on the cut cylinder.

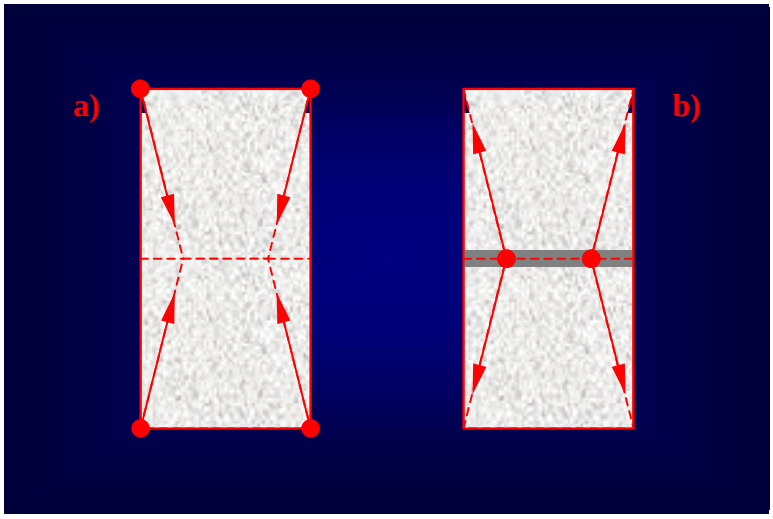

Figure 10: Crack path for the uncut (a) and the cut (b) cylinder.

The restoration of the specimen has been carried out with mortar. Since the stiffness of the grommets is much higher than the stiffness of the concrete, once loaded the specimen the three grommets have the function to concentrate the load in correspondence of their fixing points. This results in a failure mechanism with the dominant crack enucleating on the middle cross-section, starting from the fixing points of the grommets. The final failure surfaces were the same in the two cylinders.

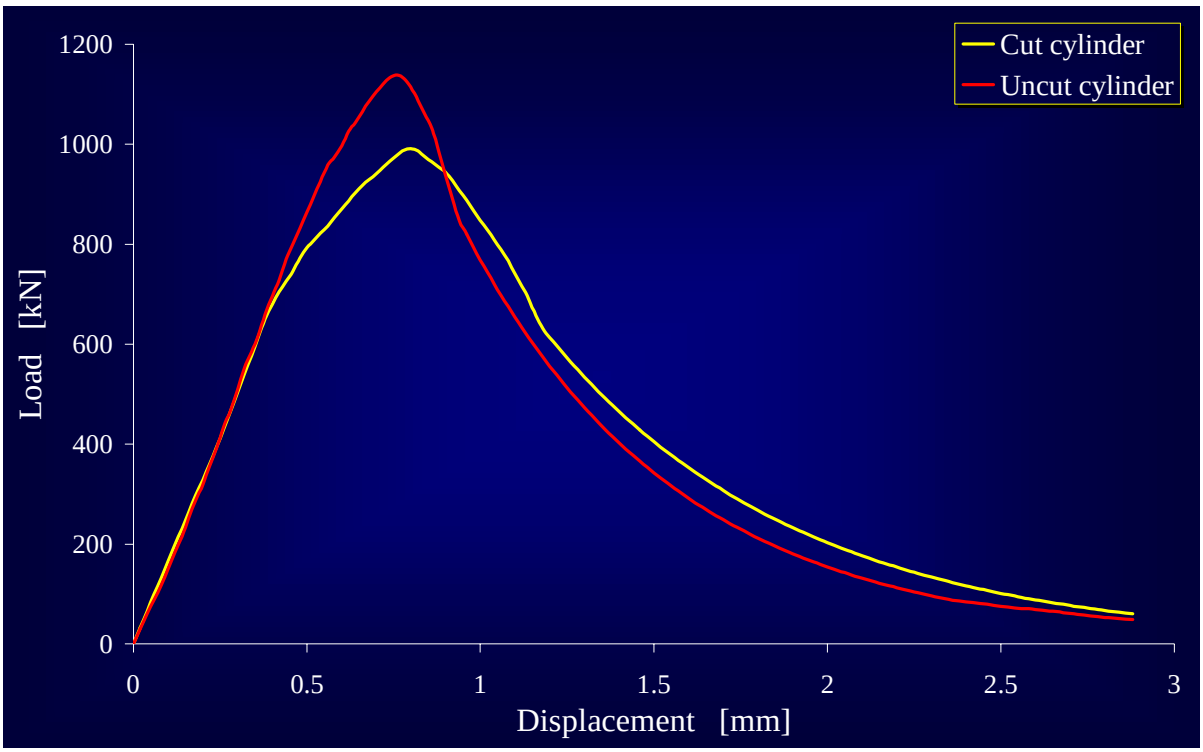

Figure 11: Load-displacement curves for the cut and the uncut cylinder.

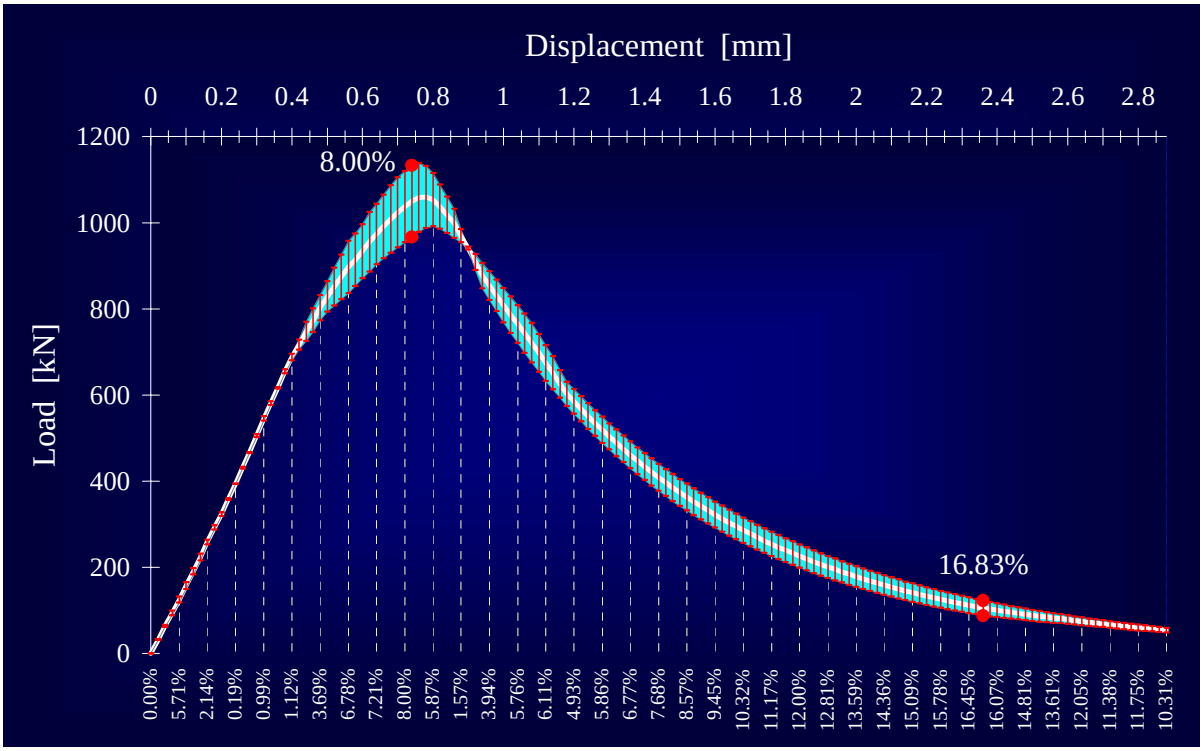

Figure 12: Percentage difference from the mean value of load, at intervals of displacement of 0.08 mm.

In Fig 11. the load – displacement experimental curves for the uncut and the cut cylinder are shown. The curves in Fig. 11 are almost superimposed as long as the dominant crack does not start to propagate. This result confirms that the initial stiffness of the restored specimen is almost the same as the initial stiffness of the uncut specimen, stating that the cut and the subsequent restoring have not significantly modified the stiffness properties of the cylinder.

When the dominant crack starts to propagate, the two curves bifurcate, assuming a different shape (Fig. 11). The presence of a point of bifurcation confirms that the failure mechanisms of the two specimens were actually different, as it was in the Authors aims.

In Fig. 12, the percentage difference from the mean value of load is quoted for intervals of displacement of 0.08 mm. The two local maximums are quoted directly on the plot. The maximum percentage difference from the mean value is reached in advanced phase of softening (Fig. 12) and is equal to about 17%. The maximum percentage difference in the neighborhood of the peak is equal to about 8% (Fig. 12).

In Fig. 13 the $\sigma_{eff} - \varepsilon_{eff}$ relationships obtained for the two tested cylinders are shown.

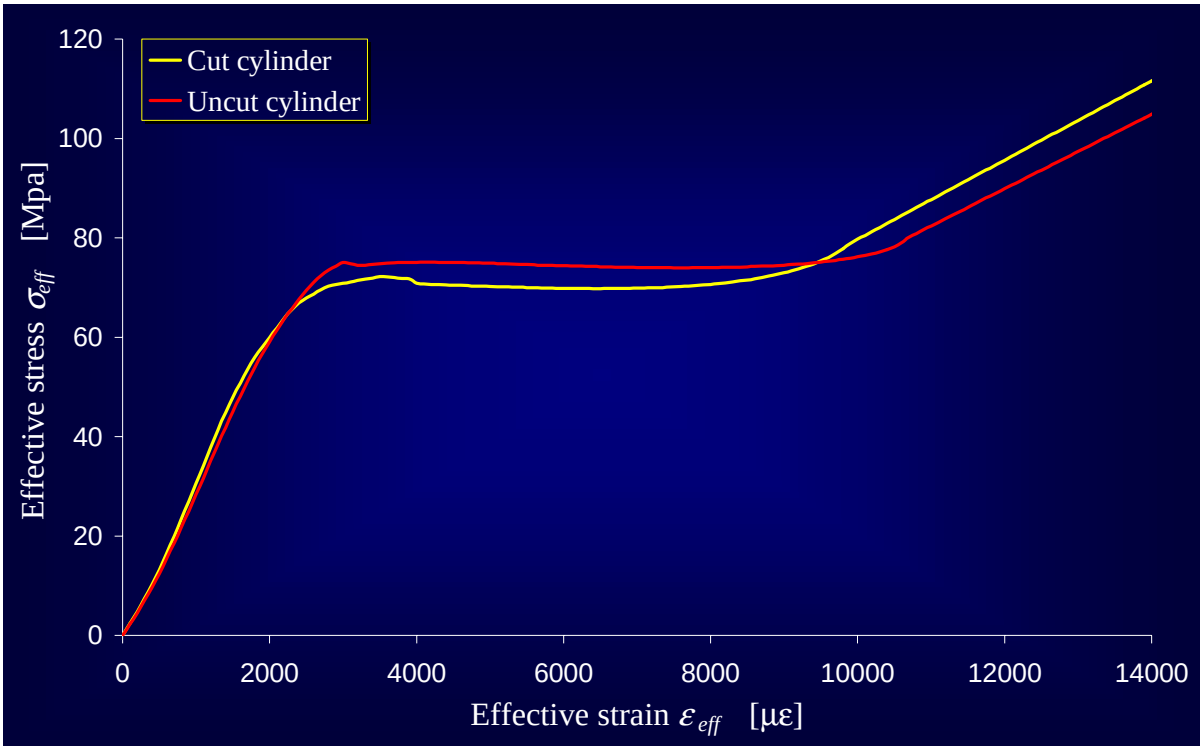

Figure 13: Effective stress-effective strain curves for the cut and the uncut cylinder.

In Fig. 14, the percentage difference from the mean value of effective stress is quoted for intervals of effective strain of 400 με. The three local maximums are quoted directly on the plot. The percentage difference for the point of the $\sigma_{eff} - \varepsilon_{eff}$ plane corresponding to the first local maximum in Fig. 12 (the point near the peak) is plotted in yellow.

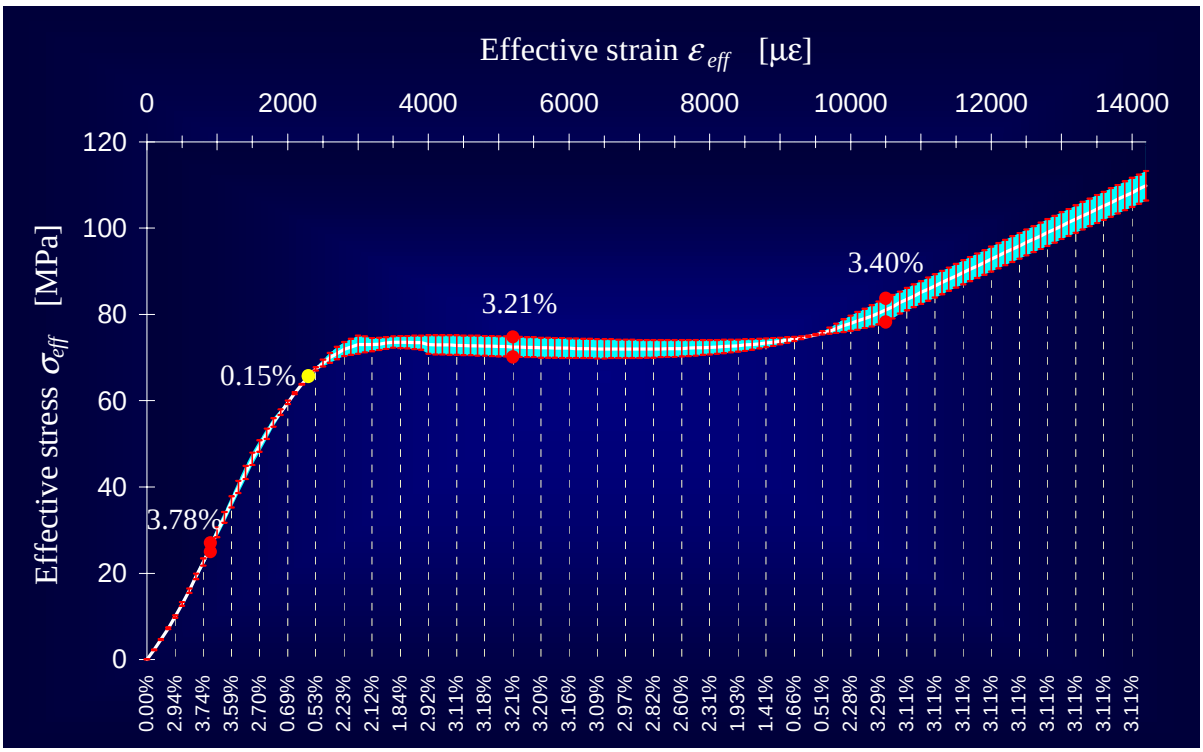

Figure 14: Percentage difference from the mean value of effective stress, at intervals of effective strain of 400 με .

As it can be appreciated in Fig. 14, the percentage difference from the mean value computed in the $\sigma_{eff} - \varepsilon_{eff}$ plane is noticeably lower than the percentage difference from the mean value computed in the $N - v$ plane.

4 Conclusions

The two identified $\sigma_{eff} - \varepsilon_{eff}$ curves do not exhibit bifurcation points. This means that the identified curve is not sensitive to the change of failure mechanism. The low value of percentage difference from the mean value in correspondence of the yellow points in Fig. 14 confirms this conclusion, since for these points the effect of the different failure mechanism reaches a maximum (Fig. 12). This result is very important to give validity to the proposed identification procedure, since the independence from the failure mechanism is one of the most important requisites for an identifying procedure of material parameters. Moreover, this result is as much important as the traditional identifying procedure for constitutive laws in uniaxial loading is not insensitive to the change of failure mechanism.

All the main results of the first experimental programme are confirmed. In particular, the $\sigma_{eff} - \varepsilon_{eff}$ relationship exhibits a positive derivative and the dispersion range is very little.

Acknowledgments

This study has been carried out with the financial support of the Italian Ministry for Universities and Scientific and Technological Research (MURST).

Profs. Erasmo Viola and Antonio Di Leo are gratefully acknowledged for their suggestions and scientific supervision.

References

[1] Ferretti, E., Modellazione del Comportamento del Cilindro Fasciato in Compressione, *Ph.D. Thesis*: University of Lecce – Italy, 2001 (in Italian).
[2] Bažant, Z.P., Belytschko, T.B. and Chang, T., Continuum Theory for Strain-Softening, *Journal of Engineering Mechanics*, Vol. 110(12), p. 1666, 1984.
[3] Ferretti, E. and Carli, R., Programma Sperimentale sul Comportamento in Compressione Monoassiale del Calcestruzzo; Parte II: Elaborazione dei Risultati Sperimentali, *Technical Note 33*, DISTART – University of Bologna – Italy, 1999 (in Italian).
[4] Rosati, G and Natali Sora, M.P., Direct Tensile Tests on Concretelike Materials: Structural and Constitutive Behaviors, *Journal of Engineering Mechanics*, Vol. 127, p. 364, 2001.
[5] Ferretti, E., Effective Properties for Plain Concrete Obtained by Uniaxially Compressed Cylinders, *submitted to Engrg. Fract. Mech*., 2002.
[6] Daponte, P. and Olivito, R.S., Crack Detection Measurements in Concrete, *Proceedings of the ISMM International Conference Microcomputers Applications*, p. 123, December 14-16, 1989.
[7] Ferretti, E., Viola, E., Di Leo, A. and Pascale, G., Propagazione della Frattura e Comportamento Macroscopico in Compressione del Calcestruzzo, *XIV AIMETA*, October 1999 (in Italian).
[8] Di Leo, A., Di Tommaso, A. and Merlari, R., Danneggiamento per Microfessurazione di Malte di Cemento e Calcestruzzi Sottoposti a Carichi Ripetuti, *Technical Note 46*, DISTART – University of Bologna – Italy, 1979 (in Italian).